J. Fluid Mech. (1996), vol. 327, pp. 199–219

An experimental study of oscillatory convection in liquid gallium

By MANFRED G. BRAUNSFURTH AND T. MULLIN†

Department of Atmospheric Oceanic and Planetary Physics, Oxford University, Parks Road, Oxford, OX1 3PU, UK

(Received 12 October 1995 and in revised form 13 June 1996)

Results are presented of an experimental study of the onset of time-dependent flows in a sample of liquid gallium subjected to a horizontal temperature gradient. The primary control parameter is the Grashof number which is set by the temperature difference. However, we have also taken the novel approach of varying the Prandtl number in a systematic way using the applied mean temperature. This has uncovered some surprising new dynamical states. Furthermore, the interaction between competing oscillatory flows has produced interesting dynamical behaviour including secondary Hopf bifurcations where both the frequency and amplitude grow from zero as the critical point is passed.

1. Introduction

The demand for homogeneous pure semiconductor crystals for use in high-density integrated electronic chips has meant that more refined crystal growing processes are required. One way of achieving this is to improve the current processes by obtaining a deeper understanding of some fundamentals of present techniques so that improvements can be found. The current state of knowledge of the many factors which determine crystal homogeneity is reviewed in articles by Brown (1989), Langlois (1985), and Pimputkar & Ostrach (1981). One of the important effects is that of convective fluid motion in the crystal melt. Thus, in the present study, we will focus on those aspects of the underlying fluid motion which will have an effect on the crystal growing process.

At certain values of the control parameters, the steady convecting fluid flow can develop an oscillation. These oscillations were first observed experimentally by Müller & Wiehelm (1964) and by Hurle (1966). It has been demonstrated that the time-dependent flow induces thermal oscillations and they in turn are one of the main reasons for the occurrence of layered variations of impurities in the crystal, known as striations. Specifically, numerical investigations by Crochet, Geyling & van Schaftingen (1983, 1987) and experimental observations by Thevenard *et al.* (1991) show that small temperature variations cause the crystal to solidify and remelt at the interface, thus creating layers of impurities.

The material we use in our experiment is gallium which is a liquid metal above 29.8°C and hence the transport of heat mainly takes place by conduction. Convective flows are also found and the main physical driving mechanism of these is buoyancy,

† Address for correspondence: Schuster Laboratory, The University of Manchester, Manchester M13 9PL, UK.

induced by temperature gradients along the melt. The experiment is a model of the horizontal Bridgman technique where a temperature gradient exists between the hot melt and the cold crystal. Buoyancy forces can lead to steady convective flows, which separate into circulating eddies. Under other circumstances they can produce time-dependent dynamics. However, the precise mechanisms which give rise to the thermal oscillations are poorly understood and it is these that will be the focus of attention of the present study.

Convective flow of a liquid metal contained in a rectangular enclosure is governed by four dimensionless parameters, namely two aspect ratios, the Grashof number and the Prandtl number. The two aspect ratios describe the geometry of the set-up: one is the ratio of the length of the container in the direction of the temperature gradient to the height $A_y = L/H$, and the second is the ratio of the width to the height, $A_x = W/H$. The Grashof number is the non-dimensional group which corresponds to the applied temperature gradient, and it is defined as $Gr = (g\alpha\Delta T H^3)/(\nu^2 A_y)$, where α is the volumeric expansion coefficient, ν is the kinematic viscosity of the fluid, g is the acceleration due to gravity, and ΔT is the applied temperature difference. The temperature, length, and time scales of the problem are $\Delta T/A_y$, H, and H^2/ν respectively. The Prandtl number relates the momentum diffusivity to the thermal diffusivity of the material, and is defined as $Pr = \nu/\kappa$, where the thermal diffusivity is given by κ.

Pioneering work in experimental investigations of the flow dynamics of liquid gallium in a rectangular enclosure of moderate aspect ratio was carried out by Hurle (1966), and by Hurle, Jakeman & Johnson (1974). Details of a more recent experimental and numerical study are given in Braunsfurth *et al.* (1995), which also contains a review of work on steady flows in the present problem. In summary, the types of fluid flows found are the following. At small temperature differences, the convective flow is steady. However, when the temperature difference is increased above a critical value, the flow was found by Hurle *et al.* (1974) to oscillate. Their investigation then concentrated on the dependence of the critical temperature difference on the aspect ratios of the system and, especially, on the strength of an applied transverse magnetic field. Their findings indicate that the critical temperature difference for the onset of oscillation decreases as the aspect ratios A_x and A_y increase. In addition, the critical temperature difference for the onset of oscillatory flow was found to be proportional to the square of the applied transverse magnetic field. The dependence of frequency of the oscillations on the aspect ratio was also investigated. The period of oscillation was found to be proportional to the length of the boat. It was noted that one of two different frequencies could appear at the onset depending on the depth of the gallium. However, this feature was not investigated in detail.

McKell *et al.* (1990) later studied a particular feature of the time-dependent dynamics. Their investigation concentrated on the parameter range close to the point where a line of secondary Hopf bifurcations giving rise to quasi-periodic motion intersects a line of period-doubling bifurcations. The point of intersection of the two lines of bifurcation points is a two-control-parameter problem and is called a codimension-2 point. (See e.g. Guckenheimer & Holmes 1983, Mullin 1993 and Wiggins 1990). McKell *et al.* (1990) were able to show the existence of a codimension-2 point and the emergence of chaos via torus doubling.

Other studies of convection in liquid metals were performed by Pratte & Hart (1990) and Hart & Pratte (1990), who investigated oscillatory convection in samples of mercury. The experimental set-up used by them consists of three separate rectangular chambers filled with mercury, of aspect ratios 1×4×1, 1×4×2, and 1×8×8, where

the aspect ratios are defined as height×length×width. The critical Grashof numbers for the onset of oscillation were found to be $Gr = 22200$ for the 1×8×8 container, $Gr = 39000$ for the 1×4×2 container, and $Gr = 135000$ for the 1×4×1 container. The non-dimensional frequency (f_N) of the oscillations based on the time scale of H^2/ν was found to be 14.3 and 43.8 for the 1×4×2 and the 1×4×1 containers respectively. At higher Grashof numbers, further oscillatory transitions were found to lead to frequency-locked states and eventually to chaos. It was noted by Pratte & Hart (1990) that in the case of the 1×8×8 chamber the frequency of the oscillation just after onset was sensitively dependent on the rate at which the Grashof number was changed, and two different frequencies of oscillation were found at the same Grashof number.

Numerical studies of convection in liquid metal flows can be sub-divided into three categories, namely two- or three-dimensional numerical integrations of the equations of motion, and stability calculations. In general, the results of different two-dimensional numerical studies are in accord with each other. This is also true for the three-dimensional numerical studies, and those of the stability analyses. However, when the results of these three different approaches are compared, then there are both quantitative and qualitative differences.

The results from the three types of studies can be summarized as follows. A large number of two-dimensional numerical studies have been carried out at an aspect ratio of $A_y = 4$, and they can be found in the collection of numerical benchmarks compiled by Roux (1990). These include work by Behnia & Davies (1990), Behnia *et al.* (1990), Ben Hadid & Roux (1990), Garrec & Magnaud (1990), and Le Quéré (1990). Other numerical results for a container of aspect ratio 4 include the studies by Crespo del Arco, Pulicani & Randriamampianina (1989), Roux, Ben Hadid & Laure (1989), Pulicani *et al.* (1990), and Okada & Ozoe (1993). A pertinent example of these studies is provided by Le Quéré (1990) who found a critical Grashof number for a Hopf bifurcation of $Gr_c = 27875$, and a non-dimensional frequency of oscillation $f_N = 17.3$. Ben Hadid & Roux (1990) found $Gr_c = 30000$ and $f_N = 20$. In both cases, the steady flow before the onset of oscillation consists of three co-rotating convection cells, and the oscillation is found to be a pulsation of these cells symmetrically about the centre point of the container.

A small number of three-dimensional numerical studies have also been performed. The first reported studies by Chabbard & Lalanne (1990), Extremet *et al.* (1990), and Gervasio *et al.* (1990) appear to be inaccurate due to insufficient grid resolution, and have been superseded by more accurate calculations by Afrid & Zebib (1990), and by Henry & Buffat (1990). Both of the latter studies consider the mathematical abstraction of a fluid of Prandtl number zero where heat transport is due to conduction alone with no contribution from the circulating fluid. Afrid & Zebib (1990) found the onset of oscillations for a container with aspect ratios $A_x = 2$ and $A_y = 4$ to be $Gr_c = 30000$ at a frequency of $f_N = 36.6$. For a container of aspect ratio $A_x = 1$, the values were $Gr_c = 125000$ and $f_N = 39$. In contrast to the two-dimensional results, Afrid & Zebib (1990) have found that the flow remains in the form of a single convection cell at all times. The work by Henry & Buffat (1990) on the other hand indicates that three cells are present. During a cycle of the oscillation, the central convection cell precesses out of the plane about the centre point of the cavity, and hence the oscillatory flow is three-dimensional in nature. Thus this type of motion cannot take place in the two-dimensional calculations.

We now turn to the stability calculations by Winters (1988, 1990), Winters & Jack (1989), and by A. C. Skeldon (private communication). The approach chosen by

these authors is different from that used in the studies discussed above, in that it uses a technique which is halfway between numerical and analytical methods. First, a finite element method is used to compute a steady base flow for the particular set of boundary conditions. Then, linear stability analysis is performed, allowing an estimate to be made of the critical parameter values for the onset of oscillations. The studies were focused on a container of aspect ratio of $A = 4$ with a two-dimensional flow field. Winters (1988) found the onset of oscillations at $Gr_c = 38085$ with a frequency of $f_N = 80.5$. The oscillation is found to be symmetric about the centre point of the container. These calculations have recently been extended by Skeldon to include the influence of the Prandtl number on the critical Grashof number for the onset of oscillations. In her study, variations in the material properties of the fluid with the local temperature were taken into account. The critical Grashof number is seen to increase in a smooth and monotonic fashion from $Gr_c = 37000$ at Prandtl number $Pr = 0.0155$ to $Gr_c = 99700$ at Prandtl number $Pr = 0.0215$.

In summary, the experimental findings and the different numerical results disagree qualitatively and quantitatively in predicting the onset of oscillations. A variety of different frequencies of oscillation are found, and the onset of oscillation is found to lie in the range $Gr = 22200$ to $Gr = 135000$, with a sensitive dependence on the aspect ratios and on the Prandtl number. However, the details of this dependence of the critical Grashof number on the other parameters of the system have not been investigated systematically other than in the preliminary work of Skeldon. Finally, the dependence on the control parameters of the nature and frequency of the oscillation is not well established.

Here we present results from a carefully controlled experimental study of the onset of oscillation in a sample of liquid gallium. We use a novel approach in treating the Prandtl number as a variable parameter whose value is adjusted using the dependence of the material properties on the mean temperature of the fluid. Thus the onset of oscillation is investigated in the plane in parameter space spanned by the Grashof number and the Prandtl number. The findings are analysed using the tools provided by bifurcation and dynamical systems theory, in order to provide a base of observations and understanding of the observed phenomena in terms of the experimental parameters.

2. Experimental set-up and properties of gallium

The experimental set-up consists of a rectangular ceramic channel which holds the liquid gallium between two conducting end plates. The channel is precision machined from pyrophyllite, which is then fired to create a hardened ceramic channel, with a thermal conductivity of 1.6 $W m^{-1} K^{-1}$. The channel has an inner width of 12.82 mm ± 0.05 mm, and a length of 38.7 mm ± 0.1 mm. As shown schematically in figure 1, the channel is covered with a ceramic lid machined from the ceramic MACOR, so that the height of the channel is 9.7 mm ± 0.1 mm, which gives an aspect ratio length/height of $A_y = 4.0$. The thermal conductivity of MACOR is 1.48 $W m^{-1} K^{-1}$, and matches that of pyrophyllite to within 8%. The thermal conductivity of both ceramics is between 18 and 29 times lower than that of gallium in the range of temperatures encountered in the experiment, and the walls and the lid are at minimum 5 mm thick. Hence the sidewalls provide a good approximation to rigid adiabatic boundary conditions. Clearly the lid cannot cover the whole of the gallium surface if measurements are to be made. Thus a thin slot is left in the lid to allow a thermocouple to be inserted into the melt at different selected positions. The slot is in the centre of the lid, and

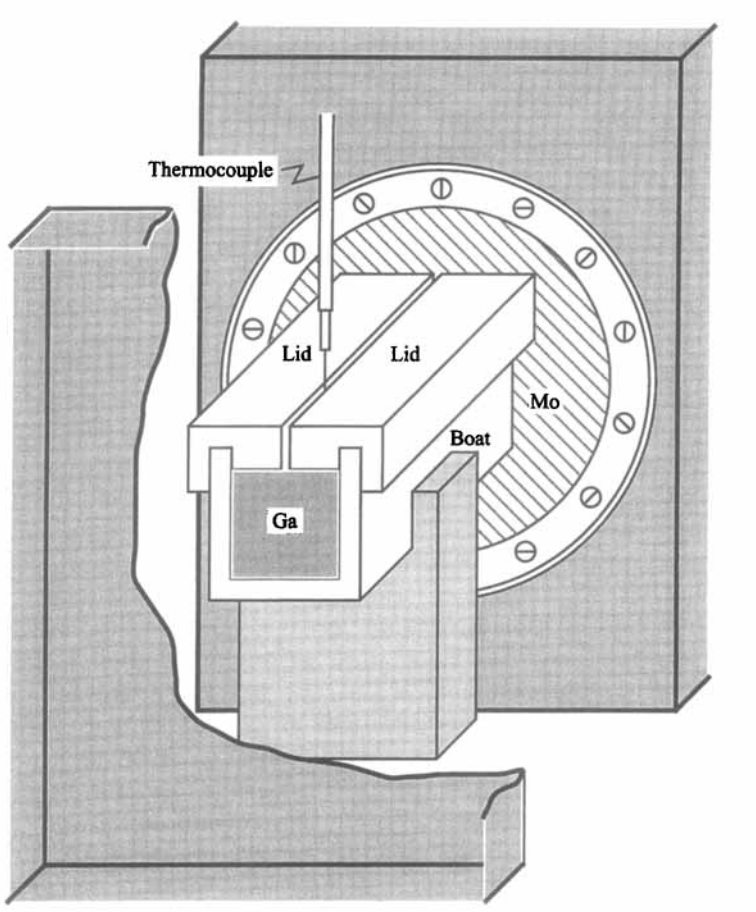

FIGURE 1. Schematic view of the experimental apparatus. The ceramic boat containing the gallium is sandwiched between temperature-controlled metal walls. The entire apparatus is mounted inside a temperature-controlled environment. Measurements are made with a thin thermocouple.

runs along the length of it, as can be seen in figure 1. The width of the slot is 0.5 mm $\pm$0.1 mm, which amounts to 4% of the width of the container. It should be noted that the lid appears to have little quantitative effect on the results. In fact, experiments performed without a lid showed only marginal differences to those with a lid. We believe this occurs because the gallium quickly forms an oxide layer which acts as a rigid boundary and is also a reasonable insulator.

The ends of the channel are defined by 1 mm thick molybdenum walls, through which the heating and cooling is applied. Molybdenum is chosen because it is one of the few metals which is reasonably resistant to attack from the liquid gallium. Circular pieces of molybdenum sheet are mounted in copper boxes, through which temperature-controlled fluid is circulated. The fluid used is silicone oil which has a viscosity 10 cS at room temperature, and it is kept at a constant temperature by Haake G8-G heating/cooling temperature controllers. The copper boxes contain 0.7 l of liquid which provides good thermal inertia, and so act as a low-pass thermal filter to damp out external temperature fluctuations. The fluid is injected into the boxes at speeds of the order of one litre per minute, ensuring turbulent mixing of the fluid inside the box, and hence providing a uniform temperature at the molybdenum wall.

In order to isolate the experiment from thermal fluctuations of the surroundings, the copper boxes are lagged in styrofoam, and the ceramic boat with the gallium is lagged with approximately 2 cm of cotton wool. In addition, the whole set-up is enclosed in a temperature-controlled air cabinet. Thermocouple probes inside the copper boxes were used to perform control measurements of the temperature of the fluid, which was found to be constant to $\pm 0.05°C$ over the period of days, at total temperature differences of up to 100°C. This indicates a level of noise of $O(10^{-3})$.

Measurements of the temperatures at different points in the gallium were made using a sheathed K-type (chromel-alumel) thermocouple. The outer diameter of the thermocouple sheath is 250 μm, ensuring that only a minimal disturbance is present in the flow. Furthermore, the thermocouple junction has a volume of $(250\ \mu m)^3$, giving a close approximation to a point measurement. The slew rate of the thermocouple allows temperature changes of up to $3\ K\ ms^{-1}$ to be measured accurately. This is an important feature when studying time-dependent phenomena. The signal from the thermocouple is processed by an amplifier, which also provides an electronic cold-junction compensation for the thermocouple signal. Both the amplifier and cold-junction reference are enclosed in an isothermal box inside the air cabinet, and the stability of the amplifiers achieved in this way resulted in fluctuations in the signal of less than 0.01°C.

The signal from the thermocouple amplifiers is conditioned by a level shifter and amplifier, and is finally sampled using a 12-bit analog to digital converter which enables the data to be stored and analysed using a personal computer. This computer is also used to control the settings of the external temperature controllers which provide the temperature gradient across the sample of gallium.

The bifurcation set depends on the aspect ratios of the system but these parameters can only be varied in discrete steps. However, the Grashof and Prandtl numbers can be controlled readily and virtually continuously by altering the temperature difference and the mean temperature applied to the gallium. The Grashof number depends on the volumetric expansion coefficient, the viscosity, and the density of the fluid, along with the applied temperature gradient. The Prandtl number depends solely on the viscosity, thermal conductivity, and specific heat. The material properties in turn vary with the local temperature, thus introducing an implicit temperature dependence to the Grashof and Prandtl numbers.

The variation of the governing parameters with temperature has far reaching consequences. On the one hand, the parameters are no longer constant over the whole system. It is hence, in principle, possible to have different dynamics in different parts of the container, such as in the case studied by Kobine, Mullin & Price (1995) of a Taylor–Couette problem with a tapered inner cylinder. However, we have been unable to find evidence for such local dynamics in our system. The approach that we have taken treats the parameters as constants over the flow region, but allows a dependence on the mean temperature in the fluid. Numerical calculations by A. C. Skeldon (private communication) suggest that this approach is a valid one, since all the flow dynamics calculated to date show that the spatial variation of the parameters has only a minimal effect on the behaviour. A more important consequence of the temperature dependence of the parameters is the fact that the parameter space is increased by an extra dimension. All of the previous experimental and numerical investigations have treated the Prandtl number as a constant. As we will see, many of the dynamics observed in the present study can only be understood if we consider the dynamics as a function of both the Grashof number and the Prandtl number.

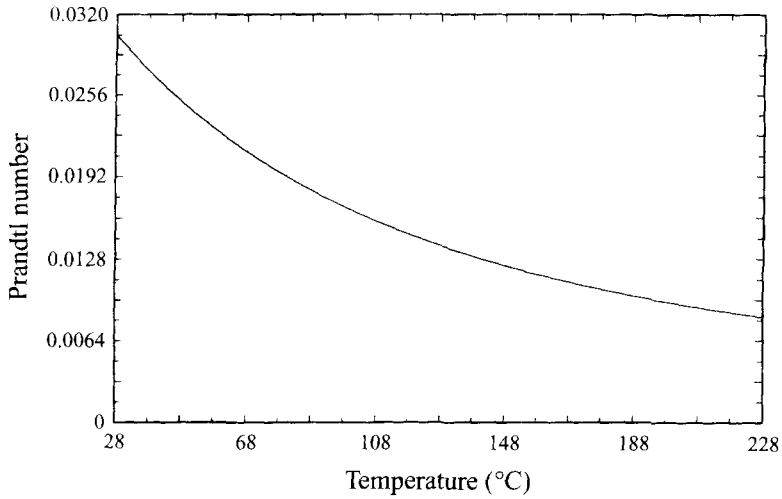

FIGURE 2. Prandtl number plotted as a function of the mean temperature in the flow.

The Prandtl number can be written as a function of the mean temperature $\overline{T}$, and its functional form is shown in figure 2. The Grashof number becomes a function of the mean temperature $\overline{T}$ and the temperature difference ΔT between the ends. The following expressions were derived using the tabulated values of the various properties of gallium found in a range of different reference works (see Hampel 1954; Lange 1967; Filyand & Semenova 1968; Hultgren *et al.* 1973; Touloukian *et al.* 1979; Kaye & Laby 1982; Weast *et al.* 1983, 1993; ASM 1990; Brandes & Brook 1992; Iida & Guthrie 1993):

$$Pr = \frac{6.135 \times 10^{-3}\, e^{(481/\overline{T})}}{1 + 4.67 \times 10^{-3}(\overline{T} - T_{melt})},$$

$$Gr = 2.4732 \times 10^{11} \left(1 - \frac{(\overline{T} - T_{melt})}{1163.5} + \frac{(\overline{T} - T_{melt})^2}{4808600}\right) \frac{\Delta T H^3}{A_y}\, e^{(-962/\overline{T})},$$

where T_{melt} is the melting point of gallium, 29.8°C.

It should be noted that the above expressions for the Grashof number and the Prandtl number are subject to large systematic uncertainties arising from errors in the values of the material properties of gallium, especially so in the case of the Prandtl number. The absolute value of the Prandtl number is only known to within 0.006, or to within 30% of its value of 0.02 at typical temperatures present in the experiment. Owing to this systematic uncertainty, it is very difficult to obtain good absolute comparison between calculation and experiment. However, the relative uncertainty is much less, and is on the order of 1%.

3. Results

We find four distinct types of temporal behaviour in different regions of Grashof–Prandtl number space, each of which corresponds to a different mode of the flow. We present the observations made in parameter ranges where different time-dependent modes interact with each other. These include the appearance of a secondary modulation of the oscillations, which is discussed in detail. It is found that the

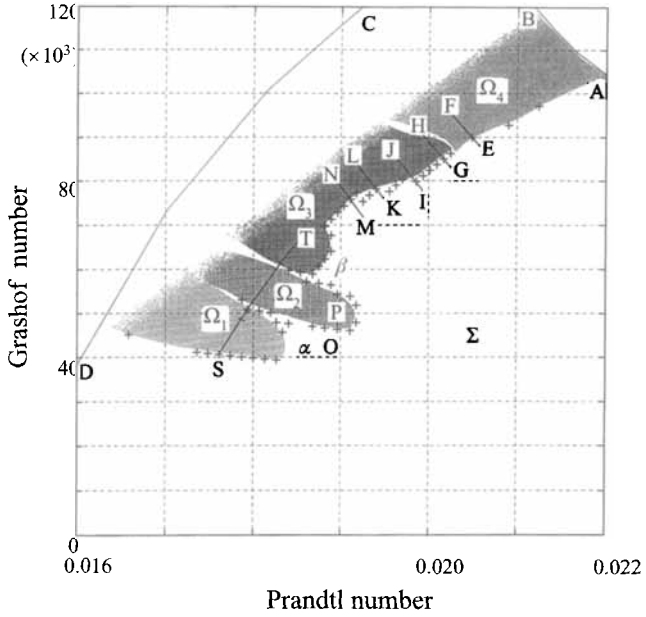

FIGURE 3. The bifurcation set of observed dynamics in Gr–Pr space. Σ denotes steady flow and the regions labelled $\Omega_1, \Omega_2, \Omega_3, \Omega_4$ indicate the parameter ranges over which the respective oscillatory states are observed. The lines labelled AB and CD mark the parameter limits of the experiment.

amplitude and the period of the secondary oscillation is strongly dependent on the control parameters, and evidence for a degenerate Hopf bifurcation is presented.

The aspect ratios of the experimental sample of gallium were $A_x = 1.3$ and $A_y = 4.0$. The main results were taken with a single thermocouple probe held at a height where the sensitive tip just pierced the top surface of the gallium. The probe was found to have no significant effect on the flow at this height, and thus it was ensured that only a minimal disturbance to the flow would be present. It was found, however, that the signal obtained from the flow at these positions is very weak, and, as we will see in the following, often has to be amplified to such a degree that the fluctuations and the noise in the experiment become apparent. The probe was placed at 10.0 mm from the cold end, which corresponds to a non-dimensional distance based on the height of the gallium of 1.03, measured from the cold end. A second probe was also used on occasions and was located at a distance of 5 mm from the hot end. All oscillations detected in the signal from the first probe were also found at the second one and vice versa. In addition there was a fixed phase relationship between the signals indicating that all the oscillations were of a global nature, i.e. the system oscillates as a whole.

An overview of the observed bifurcation set in Gr–Pr space is presented in figure 3. The different shaded regions correspond to the qualitatively distinct dynamical behaviour of the system bounded by the loci of measured bifurcation points. The curves AB and CD denote the upper limit of the range of achievable parameters with the present experimental set-up. It is limited at the high Prandtl number end by the solidification point of the gallium, and the largest Grashof number and the lower limit on the Prandtl number are determined by the maximum temperatures which can be achieved using the temperature controllers. The system was found to be symmetric with respect to a reversal of the temperature gradient, and hence negative Grashof numbers were not included in the graph.

The flow is steady in the region labelled Σ below the loci of critical points in figure 3. Furthermore, this steady flow comprises three co-rotating cells and is the same primary solution in the whole of the area Σ, and no evidence for sudden transitions or hysteresis effects was found in the steady-state temperature. In the mathematical abstraction of an infinite layer, we would expect a bifurcation from a parallel flow to stationary steady rolls to take place in the area Σ. However, since the experimental container is finite and of a relatively small aspect ratio $A_x = 4$, this transition is no longer a bifurcation, but a smooth development of the three co-rotating cells. A more detailed discussion of the steady flow structure and comparison with numerical results is given in Braunsfurth *et al.* (1995).

All the experimental points shown in figure 3 thus lie on the limit of stability of the same steady flow solution. They were obtained in the following way. For each point, an estimate of the range in which the bifurcation takes place is found by determining a point at which the system oscillates and one at which the flow is steady. The range thus determined is then divided into steps of 0.7°C in the temperature difference and 0.35°C in the mean temperature. At each of these steps, it was observed if oscillations of the temperature would grow or decay to below the noise level over a period of 30 minutes. Repeated measurements of the bifurcation points were found to give identical results, and the loci of the transitions were found to be independent of the history of the system.

In addition to these measurements, sets of more detailed samples were taken along the lines marked EF, GH, and so on to OP in figure 3, in order to establish whether the oscillations arise through a Hopf bifurcation. Along each of the lines, sets of samples were taken at temperatures which correspond to uniform steps along the line. The temperatures were set under computer control and each of the steps corresponds to a change in the mean temperature of 0.17°C ±0.04°C and in the temperature difference of 0.34°C ±0.08°C. At each step, a power spectrum of the measured time series was formed, and the power of the most significant peak in the spectrum corresponding to the frequency of the oscillation was determined. Thus it was possible to investigate how the power of the signal behaved close to the bifurcation point. In the case of a supercritical Hopf bifurcation, a linear measure of the amplitude of oscillation should scale as the square root of the parameter close to the bifurcation point, as discussed for example by Bergé, Pomeau & Vidal (1984). The power in the oscillation is a squared measure of the flow, and one would hence expect a linear increase in the power as a function of the parameter near the the critical point. Also, the frequency of the oscillation which arises at a Hopf bifurcation should be constant for supercritical values of the parameter.

The behaviour of the power close to the bifurcation point for the onset of oscillation of the four different oscillations is shown in figure 4. In order to normalize the graphs so that they can be presented in a single plot, the Grashof number in the scans across the bifurcation was rescaled in terms of the critical value at the bifurcation point. Since the absolute values of the power of the oscillation depends on the particular settings in the amplifying electronics, and also on the signal strength at the measurement position in the melt, power measurements only have meaning when seen relative to other measurements from the same scan. Thus power was rescaled to collapse the straight lines from each scan onto a single line. It can be seen in the plot that the power of oscillation is zero to within the experimental accuracy for all values of the parameter below the bifurcation point. After the bifurcation point, the power is seen to increase linearly with the parameter and the frequency of oscillation was found to be constant to within 3% over the range of Grashof numbers

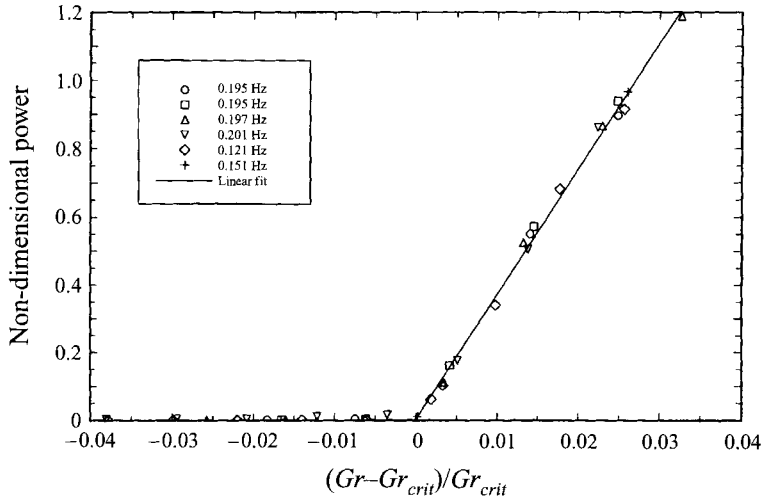

FIGURE 4. Non-dimensionalized power of the respective oscillations close to the bifurcation points.

displayed in figure 4. Both of these observations are consistent with a supercritical Hopf bifurcation.

The line of critical points in Grashof–Prandtl number space does not indicate a smooth dependence on the control parameters, but displays three significant 'bulges' around Prandtl numbers of 0.018 to 0.019. These are separated by two cusps, labelled α and β in figure 3. The system was found to evolve into four distinct types of oscillations, labelled Ω_1, Ω_2, Ω_3, and Ω_4. In each case, the frequency of oscillation was determined using a power spectrum of a sample time series. We find that the 'bulges' in the line of critical points correspond to the regions where the oscillations Ω_1, Ω_2, and Ω_3 are found, and that the cusps α and β are at the points where the different solutions meet. These observations can be understood in terms of four different modes Ω_1 to Ω_4 which become unstable in the different regions of parameter space. The nature of each of these four modes will now be described, followed by a discussion of the modal interaction which takes place at the cusps α and β.

The area labelled Ω_1 in figure 3 is a region where the system develops an oscillation with period of 6.62 s, or a frequency of 0.151 Hz, which can be non-dimensionalized with the viscous diffusion time scale H^2/ν to give $f_N = 52.1$. A sample of this oscillation was taken at a Grashof number of 46 900 and a Prandtl number of 0.0184 and its autocorrelation is given in figure 5(*a*). The x-axis of the graph gives the delay time, and the value of the autocorrelation function is plotted on the y-axis. The maxima in the autocorrelation function occur at a delay time which corresponds to an integer shift of cycles of the oscillation, and hence it can also be used to obtain an estimate of the period of the oscillation. The autocorrelation function in this case indicates a simply periodic flow, but it also shows a drop of amplitude of the function to 60% of the full range. This drop indicates the presence of an uncorrelated component in the signal, and is due to a combination of instrumentation noise and thermal fluctuations. The amplitude of the oscillation detected in the signal is 0.02°C which is of thus of the same order of magnitude as the thermal fluctuations introduced in the control of the boundary conditions.

In figure 5(*b*) we present the autocorrelation function for the second oscillatory state Ω_2, at a Grashof number of 54 100 and a Prandtl number of 0.0186. A typical

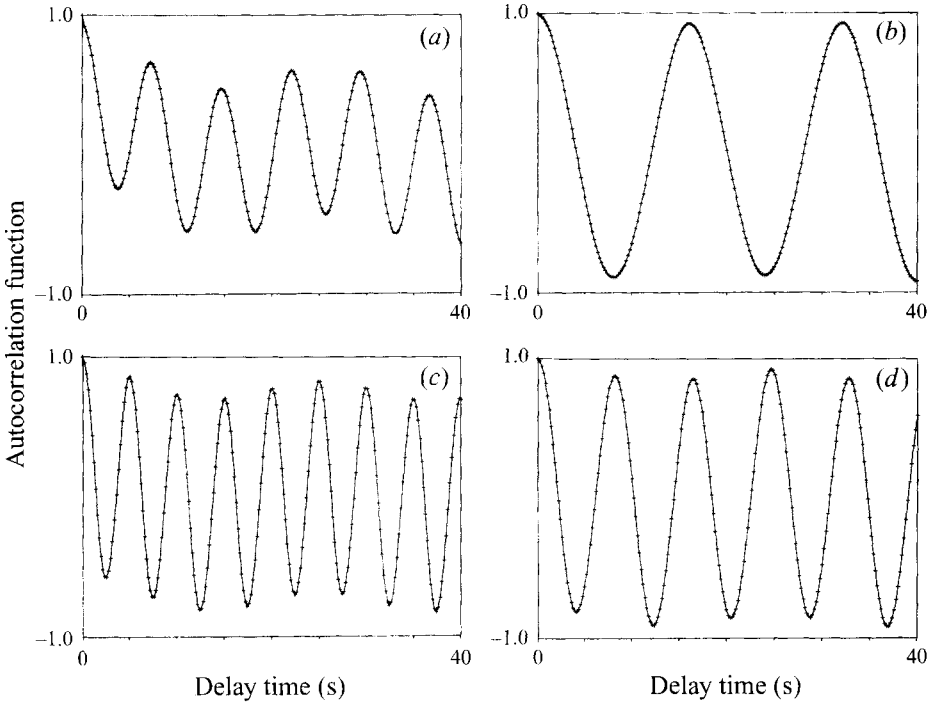

FIGURE 5. Autocorrelation function for the oscillations. (*a*) Ω_1; (*b*) Ω_2; (*c*) Ω_3; (*d*) Ω_4.

amplitude of this oscillation was found to be 0.08°C. The autocorrelation function does not show a significant decay, which indicates that the motion is singly periodic, with only a small component of instrumentation noise present. The area marked Ω_2 in figure 3 indicates the parameter range over which this oscillation is found. The frequency of oscillation is 0.0623 Hz, giving a period of 16.1 s and a non-dimensional frequency of $f_N = 21.1$.

In the region in figure 3 marked Ω_3, the oscillation has a period of 5.13 s, or a frequency of 0.195 Hz, and a non-dimensional frequency of $f_N = 65.7$ with a typical amplitude of oscillation of 0.06°C. The autocorrelation function of this oscillation is shown in figure 5(*c*). It was taken at a Grashof number of 83 500 and a Prandtl number of 0.0192. As before, the autocorrelation function can be used to confirm the period of the oscillation, and it again indicates a simple periodic thermal oscillation in the flow.

Finally, the area marked Ω_4 denotes a parameter range where the flow oscillates with a frequency of 0.121 Hz, corresponding to a period of 8.26 s and a non-dimensional frequency of $f_N = 39.2$, and an amplitude of 0.09°C. In figure 5(*d*), we present the autocorrelation function for this oscillation, sampled at a Grashof number of 94 600 and a Prandtl number of 0.0203.

We now consider the events which take place when a change in the parameter gives rise to a transition between oscillatory states. In order to investigate this, detailed sets of samples were taken along the parameter path ST indicated in figure 3, in the following way. Starting at S a set of 20 000 samples was taken over a period of 67 minutes. The temperature of the cold end was adjusted to a new value, and the system was allowed 30 minutes to settle down from the change of the parameters. Then the next set of samples was taken, and so on. The line ST was hence divided into 30

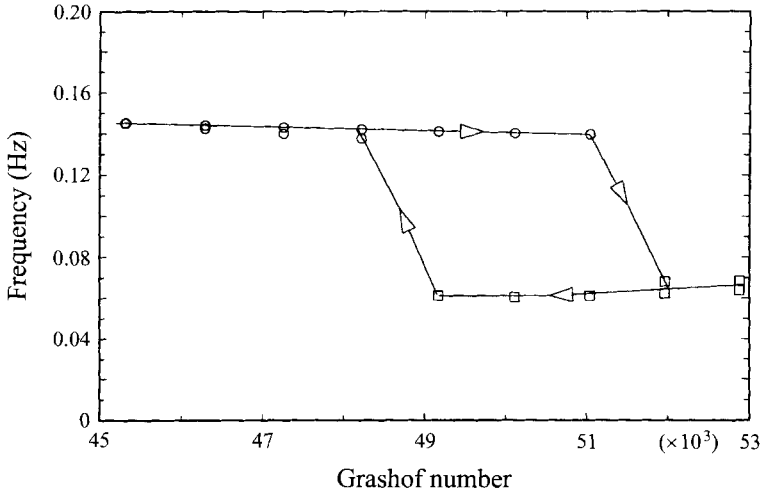

FIGURE 6. Plot of frequency versus Grashof number for the exchange between the Ω_1 and Ω_2 oscillatory states showing hysteresis.

steps, each corresponding to a change in the mean temperature of 0.17°C ±0.04°C and in the temperature difference of 0.34°C ±0.08°C. With each of these steps, both the Grashof number and the Prandtl number change. However, since the changes are predominantly in the direction of Grashof number, we choose to display the results as a function of Grashof number, and take it as understood that the Prandtl number changes in accord with the line ST in figure 3. Once such a scan was complete in one direction in parameter space, it was repeated in the opposite direction, in order to investigate the possibility of hysteresis. The temperatures were set under computer control, in order to ensure accurate and repeatable measurements.

A detailed view of the transition process between the solutions Ω_1 and Ω_2 is shown in figure 6. If the Grashof number is such that the main oscillation is Ω_1 and the Grashof number is then increased, the Ω_1 oscillation remains up to a Grashof number of 51 000. If the Grashof number is then increased by a single step then the system makes a catastrophic transition to Ω_2. On the other hand, if the initial state of the system is in the region with oscillation Ω_2, the Grashof number has to be reduced to below 49 000 before the system jumps back to Ω_1. This hysteresis cycle is indicated by the arrows in figure 6. The power spectra of the time series sampled just before and after the transition from Ω_2 to Ω_1 are shown in figures 7(*a*) and 7(*b*) respectively. It should be noted that the peak in figure 7(*a*) which corresponds to the second harmonic of the main oscillation is at a different frequency to that of the main oscillation in figure 7(*b*). The power spectra of the samples just before and after the reverse transition from Ω_1 to Ω_2 show very similar results. Thus the time series sampled just before and after the transitions only show simply periodic behaviour, and there is no evidence for interaction between these solutions. The possibility that an interaction takes place over a very small range of parameters is of course a possibility but we believe this to be unlikely. Thus the experimental results suggest that any secondary Hopf branches which arise out of an interaction must be unstable and are hence not observed.

The transition between the solutions Ω_2 and Ω_3 occurs through a different mechanism to the one described above. In figure 8, we present a graph of the frequency of oscillation against the Grashof number, which was produced in a similar way to

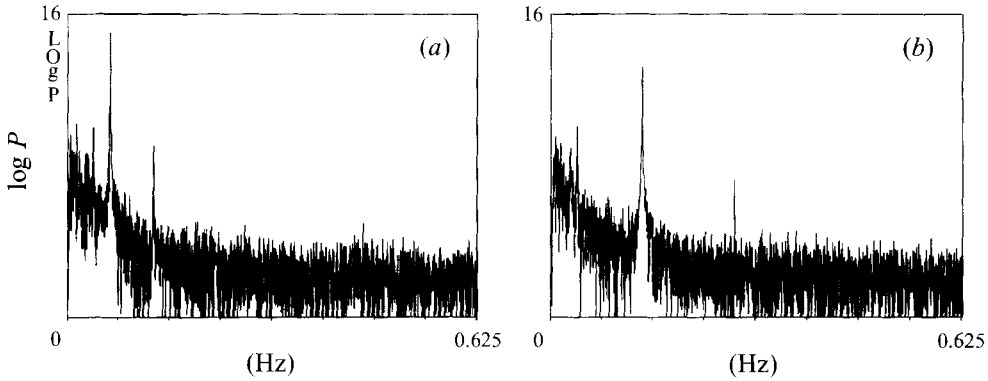

FIGURE 7. Power spectrum of the oscillation (*a*) Ω_2 just before the transition to oscillation Ω_1, and (*b*) Ω_1 just after the transition from oscillation Ω_2.

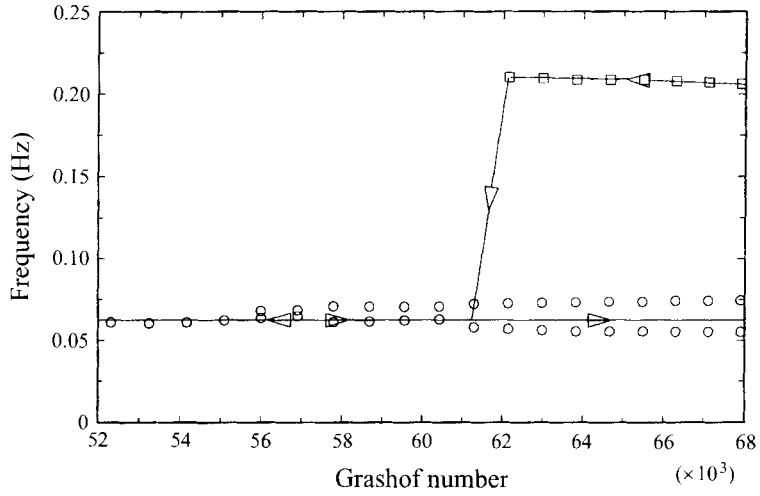

FIGURE 8. Plot of frequency versus Grashof number for the exchange between the Ω_2 and Ω_3 oscillations. The overlap of the two branches indicates the presence of hysteresis in this interaction. Note that the lower branch shows a splitting which corresponds to the onset of a quasi-periodic flow through a secondary Hopf bifurcation.

figure 6. If the system was started at the position labelled T in figure 3 in the Ω_3 solution, the Grashof number then has to be reduced to a value below 62 000 before a sudden transition to the weakly modulated Ω_2 state is found. Here, the Ω_2 solution consists of an oscillation with a period of 16 s. In addition, a modulation frequency is present on the signal and this changes in both frequency and amplitude as the Grashof number is varied. The onset and the development of this modulation will be discussed in more detail below. The modulation decays smoothly upon further reduction of the Grashof number until it is in the singly periodic Ω_2 state at a Grashof number of 55 300. No hysteresis was observed in the onset of the modulation. In the reverse direction of increasing Grashof number, the system remains in the modulated Ω_2 state for Grashof number up to and beyond a value of 68 000, which is well inside the region of stability of the oscillation Ω_3. The modulated signal consists of two frequencies at widely different time scales, which creates a double peak in the power spectrum at the mean frequency plus and minus half the lower frequency.

This spectral doublet is evident in figure 8 in the form of the splitting of the lower branch for Grashof numbers greater than 56 000. The upper limit of stability of the modulated solution has not yet been found, and we have not observed the transition back to the solution Ω_3.

4. The onset of modulation via a degenerate Hopf bifurcation

If the system is initialized in the Ω_2 state along the path ST in figure 3, and the Grashof number is then increased beyond a value of 55 000, a modulation of the periodic oscillation appears, as discussed above. The modulation has a long period when it first appears, at a Grashof number of 55 600 where the period is 216 s, and it decreases as the Grashof number is increased further. The period saturates at a value of 60 s once the Grashof number is increased beyond 60 000. The frequency close to the bifurcation point is not constant, as was the case for the Hopf bifurcations discussed above, but it now varies by a factor of nearly four over an $\approx 3\%$ change in Grashof number. The amplitude of the modulation also varies close to the bifurcation point, so that the modulation starts with zero amplitude and increases in strength as the Grashof number is increased. Three detailed scans were performed along the line ST in parameter space in figure 3, one in the direction of increasing Grashof number, and the remaining two in the direction of decreasing Grashof number. The measurements suggest that no hysteresis is present, and hence the results from all three measurements are treated on an equal basis. We propose that this scenario could be due to a degenerate Hopf bifurcation.

The period of the fast oscillation is 14 s, whereas the period of the slow oscillation has values up to 216 s. It was found that these greatly disparate time scales could not be separated satisfactorily using the spectral analysis, since the onset of the modulation was represented by the development of a large number of sidebands on the peak corresponding to the fast frequency. The power of the modulation frequency is hence distributed in many different peaks in the power spectrum. We found that representing the data in the form of the autocorrelation function was much more useful in practice. Hence this technique was used to determine the amplitude and frequency of the modulation close to the bifurcation in the following way. The time interval and amplitude of each of the maxima of the fast oscillation of the autocorrelation function was recorded. Another pass was then made through the recorded values of the maxima of the fast oscillation, to determine the maximum and minimum value of these. The difference between the maximum and the minimum of the maxima hence gives an estimate of the amplitude of the envelope, and the time interval between them gives a measure of the period of the modulation.

The results of the analysis of the amplitude and the frequency of the modulation are displayed in figures 9(*a*) and 9(*b*) respectively. It may be seen that the amplitude rises steeply close to the bifurcation point and then saturates around 0.04. It is clear from the graph that the bifurcation point lies between the last zero value of the amplitude and the first non-zero modulation, i.e. between the Grashof numbers 54 700 and 55 600. If we use the first two non-zero data points to make a linear extrapolation of the bifurcation point, we obtain a value of the critical Grashof number of 55 300. The frequency of the modulation is plotted in figure 9(*b*), as a function of Grashof number. A dotted line has been drawn at the critical Grashof number of 55 300. The results indicate that the bifurcation takes place at a point where the frequency has a small but non-zero frequency, of around 0.004 Hz. As the parameter is increased beyond the bifurcation, the frequency first grows in a fashion which is faster than

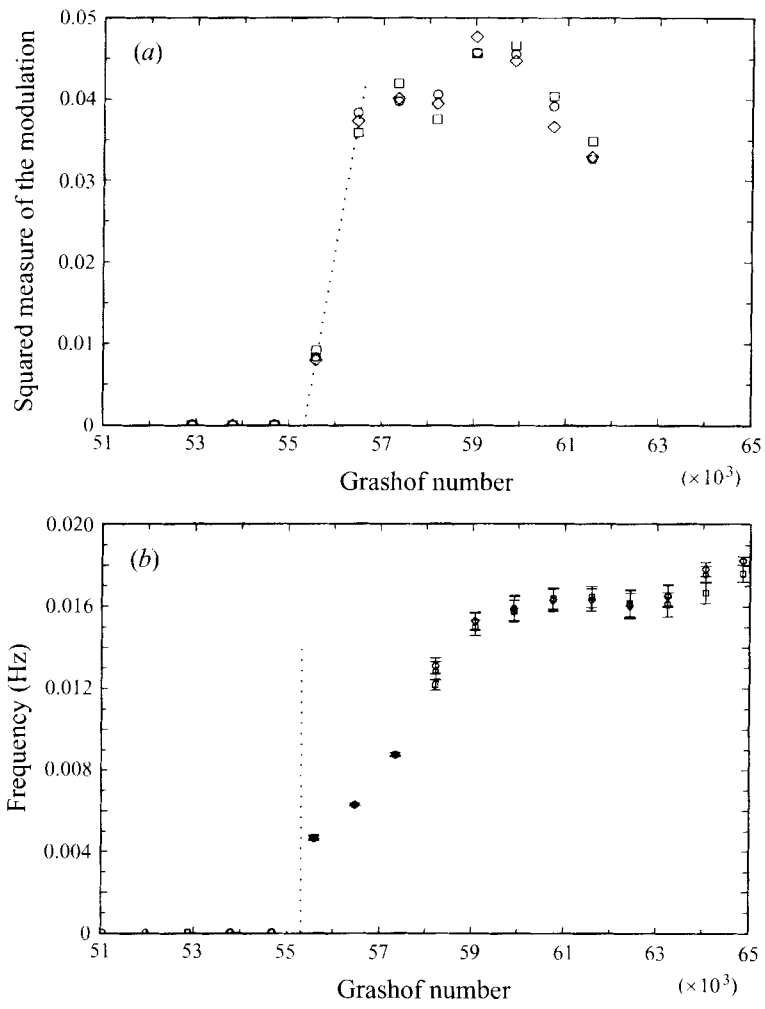

FIGURE 9. Graphs of (*a*) the squared amplitude and (*b*) the frequency of the modulation of the Ω_2 state close to the secondary Hopf bifurcation point.

linear, then the growth becomes weaker, and the frequency finally saturates at a value of around 0.016 Hz. This observation of a dramatic change in the frequency of oscillation is in stark contrast with the more usual Hopf bifurcation, where the frequency is expected to be constant close to the bifurcation point.

We now present an evaluation of the dynamics at fixed parameter values as the bifurcation is crossed. For each step, the dynamics of the system is displayed in the form of the time series and phase portrait, as shown in figures 10 to 13.

The plots consist of a time series, reconstructed phase portrait and Poincaré section obtained from the respective temperature measurements. In the time series plots, two consecutive sections of the sampled signal are displayed one on top of the other. Time runs along the x-axis, starting at the lower left corner, and progressing towards the right and up. The signals were all sampled at a frequency of 5 Hz. The phase portraits were reconstructed from the time series using the reconstruction technique based on discrete singular value decomposition, as proposed by Broomhead & King (1986) and by Broomhead & Jones (1989). The main feature of singular value decomposition

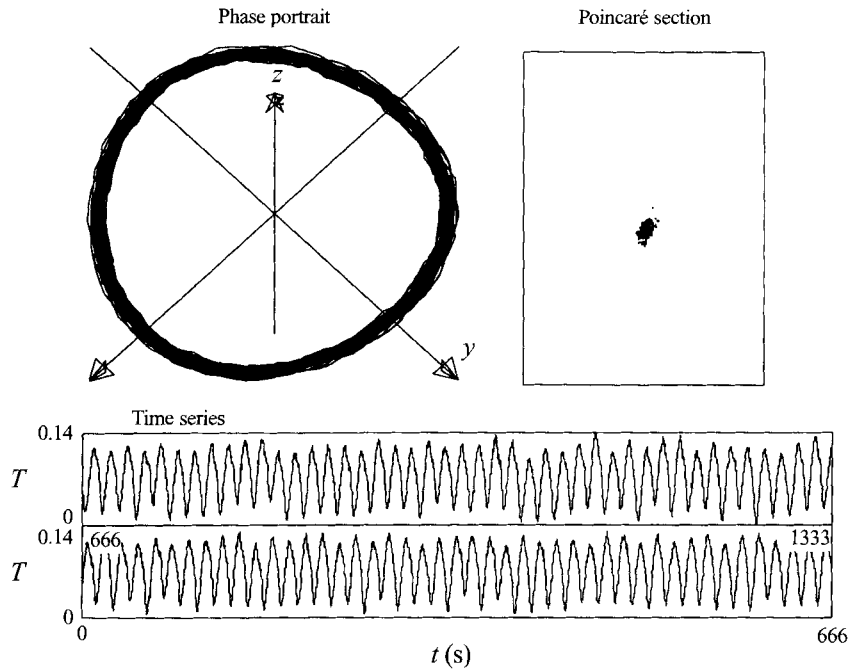

FIGURE 10. Time series, reconstructed phase portrait and Poincaré section of the oscillation Ω_2 before the onset of a modulation at a Grashof number of 54 700.

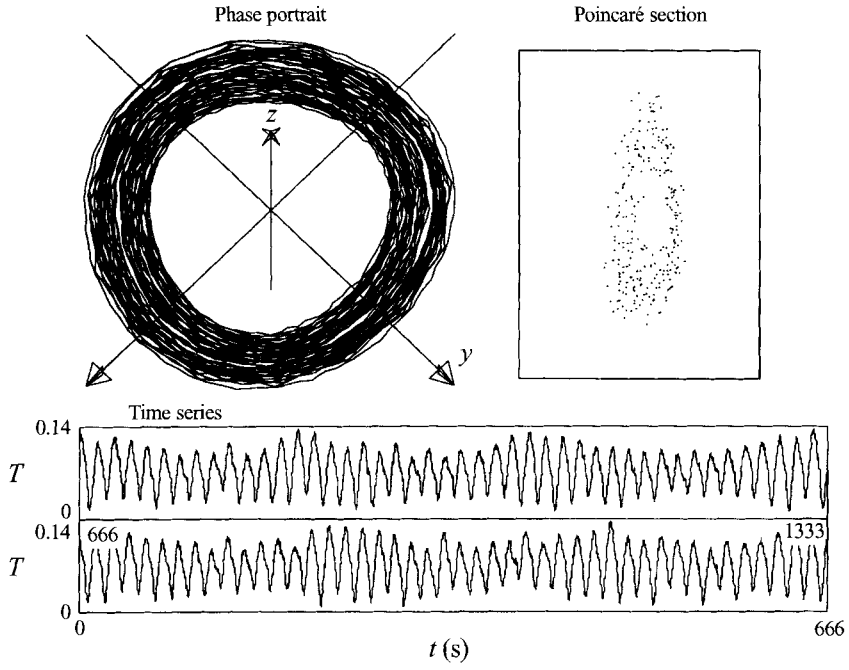

FIGURE 11. Time series, reconstructed phase portrait and time Poincaré map of the oscillation Ω_2 just after the onset of a modulation at a Grashof number of 55 600.

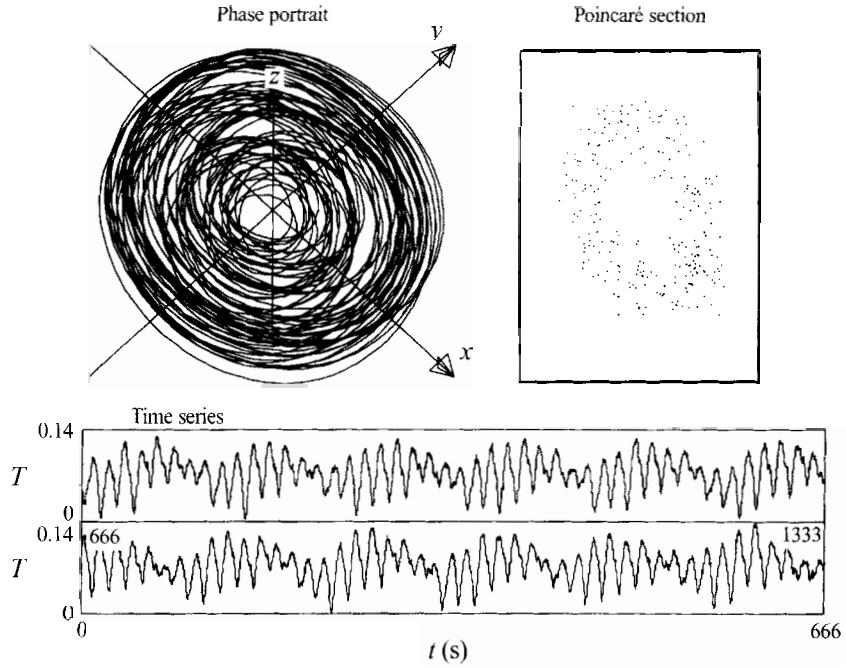

FIGURE 12. Time series, reconstructed phase portrait and Poincaré map of the modulated Ω_2 oscillation at a Grashof number of 57 300.

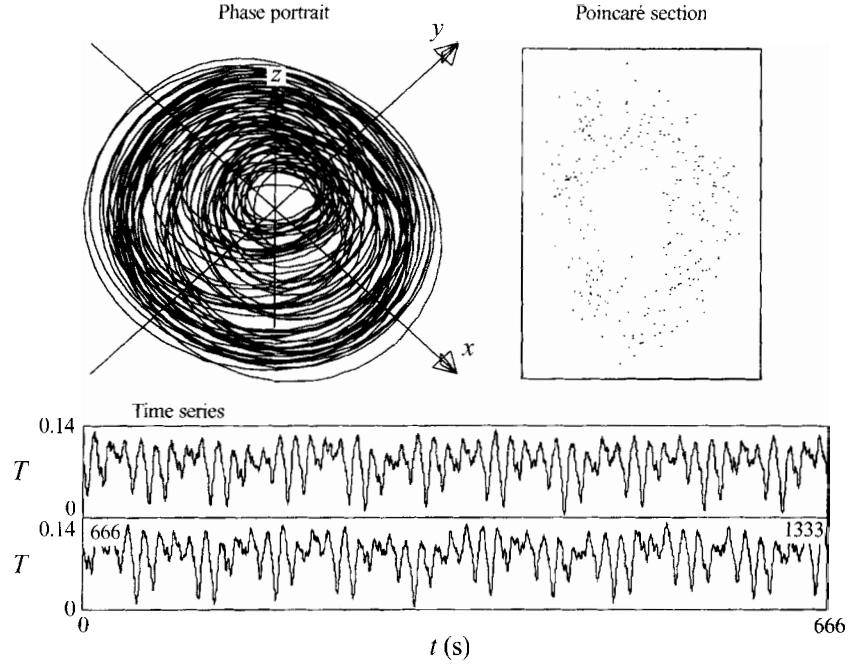

FIGURE 13. Time series, reconstructed phase portrait and Poincaré map of the modulated Ω_2 oscillation at $Gr = 61\,600$.

is that it allows the extraction of the most significant modes of oscillation from a time series, and hence enables us to reconstruct a phase portrait in the three most significant dimensions of phase space. The three axes of the phase portrait hence correspond to the three most significant components of the signal.

At a Grashof number of 54 700, the system oscillates with a single frequency; a time series sequence of this behaviour is displayed in figure 10. The system evolves along a single closed loop in phase space as indicated in the corresponding phase portrait and its Poincaré section. This fact confirms the presence of a single frequency, and there is no evidence for modulation of the signal.

When the Grashof number is increased to 55 600, so that the secondary bifurcation point is passed, the time series develops a modulation which is shown in figure 11. The modulation is evidence that a second frequency of oscillation is present in the system. Moreover, the modulation is regular so that the flow is quasi-periodic. The corresponding phase portrait now has the form of a torus where the two winding directions correspond to the two frequencies and the filled in Poincaré section provides evidence that they are not rationally related.

At a Grashof number of 57 300, the frequency of the modulation has increased, as has its amplitude. The time series, phase portrait and Poincaré section presented in figure 12 indicate that the modulation is now faster and stronger than at a Grashof number of 55 600, and that the modulation is still regular. Further increase in the Grashof number results in a further increase in the frequency of modulation, until it finally saturates at a period of 60 s. The time series of the signal at a Grashof number of 61 600 together with the corresponding phase portrait and Poincaré section are given in figure 13. The dynamics displayed in this sample is typical of that encountered in the remaining sets of samples at larger Grashof number along the scan in parameter space.

In the case of a normal Hopf bifurcation a pair of complex-conjugate eigenvalues cross the imaginary axis, as discussed by Bergé *et al.* (1984) and by Guckenheimer & Holmes (1983). The imaginary parts of these eigenvalues correspond to the frequency of the oscillation, and in general will not depend strongly on the parameter close to the bifurcation point. In contrast to that, in the present case the frequency just after the bifurcation is very small, and grows as a function of the excess parameter. This behaviour more closely resembles the cases of low-frequency periodic bifurcations studied by Davis & Rosenblat (1977), who investigated model systems of differential equations with square root or linear growth of the frequency as a function of the parameter. The occurrence of this special type of periodic bifurcation may be due to Hopf–Hopf interactions taking place at the codimension-2 point where the line of Hopf bifurcations for the oscillation Ω_2 intersects that of Ω_3. Such codimension-2 points are organizing centres for the dynamics in parameter space, and can give rise to a rich range of phenomena, as discussed by Golubitsky & Langford (1981), van Gils, Krupa & Langford (1990) and Mullin (1993).

5. Conclusions

The study of free convection in molten gallium is of widespread interest both because of its scientific importance and also its practical value as a prototype model of the Bridgman crystal growing technique. We have carried out a systematic experimental study of some interesting time-dependent phenomena in this flow using a novel approach of varying both the Grashof and Prandtl numbers. This has uncovered the surprising result that the qualitative nature of the dynamics can change

with Prandtl number. Each oscillatory state bifurcates through a Hopf bifurcation from the same steady state but the set of bifurcations does not show a smooth dependence on the control parameters.

The interaction between the different types of oscillatory motion can lead to abrupt changes in the dynamical motion as the control parameters are change smoothly. More interestingly perhaps is that another type of interaction has been uncovered which proceeds through a degenerate Hopf bifurcation where both the amplitude and frequency go to zero at the critical point. The roots of the latter phenomenon lie in a codimension-2 point. Such points are known from previous studies of fluid mechanical phenomena to form organizing centres for global dynamical motion and hold the key to a deeper understanding of more complicated behaviour including chaos.

We express warm thanks to Keith Long, for his skill and expertise in the design and construction of the experimental apparatus, to Dr A. C. Skeldon, for useful discussion on numerical calculations for the present problem, and to Drs D. S. Broomhead and D. T. J. Hurle for their helpful suggestions and discussions. M.G.B. was supported by a studentship from the Defence Research Agency at Great Malvern, UK.

REFERENCES

ASM INTERNATIONAL 1990 *Metals Handbook*, 10th edn. , vol. 2. ASM.

AFRID, M. & ZEBIB, A. 1990 Oscillatory three-dimensional convection in rectangular cavities and enclosures.*Phys. Fluids* A **2**, 1318–1327.

BEHNIA, M. & DAVIES, G. DE VAHL 1990 Finite mesh solutions using stream function–vorticity formulation. In *Numerical Simulation of Oscillatory Convection in Low-Pr Fluids* (ed. B. Roux). Notes on Numerical Fluid Mechanics, vol. 27, pp. 11–18. Vieweg.

BEHNIA, M., DAVIES, G. DE VAHL, STELLA, F. & GUJ, G. 1990 A comparison of velocity-vorticity and stream function-vorticity formulations for Pr=0. In *Numerical Simulation of Oscillatory Convection in Low-Pr Fluids* (ed. B. Roux). Notes on Numerical Fluid Mechanics, vol. 27, pp. 19–24. Vieweg.

BEN HADID, H. & ROUX, B. 1990 Buoyancy-driven oscillatory flows in shallow cavities filled with low-Prandtl number fluids. In *Numerical Simulation of Oscillatory Convection in Low-Pr Fluids* (ed. B. Roux). Notes on Numerical Fluid Mechanics, vol. 27, pp. 25–34. Vieweg.

BERGÉ, P., POMEAU, Y. & VIDAL, C. 1984 *Order within Chaos*. John Wiley & Sons / Hermann.

BRANDES, E. A. & BROOK, G. B. (eds.) 1992 *Smithells Metals Reference Book*, 7th edn. Butterworth/Heinemann.

BRAUNSFURTH, M. G., SKELDON, A. C., JUEL, A., MULLIN, T. & RILEY, D. S. 1995 Free convection in liquid gallium. *J. Fluid Mech.* (submitted).

BROOMHEAD, D. S. & JONES, R. 1989 Time series analysis. *Proc. R. Soc. Lond.* A **423**, 103–121.

BROOMHEAD, D. S. & KING, G. P. 1986 Extracting qualitative dynamics from experimental data. *Physica* D **6**, 217–236.

BROWN, R. A. 1989 Theory of transport processes in semiconductor crystal growth. *Adv. Chem. Series* **221**, 35–103.

CHABBARD, J. B. & LALANNE, P. 1990 Application of the N3S Finite Element Code to simulation of oscillatory convection in low Prandtl fluids. In *Numerical Simulation of Oscillatory Convection in Low-Pr Fluids* (ed. B. Roux). Notes on Numerical Fluid Mechanics, vol. 27, pp. 163–170. Vieweg.

CRESPO DEL ARCO, E., PULICANI, P.-P. & RANDRIAMAMPIANINA, A. 1989 Complex solutions and hysteresis cycles near the onset of oscillatory convection in a Pr=0 liquid submitted to a horizontal temperature gradient. *C. R. Acad. Sci. Paris* **309**, Série II, 1869–1876.

CROCHET, M. J., GEYLING, F. T. & SCHAFTINGEN, J. J. VAN 1983 Numerical simulation of the horizontal Bridgeman growth of a Gallium Arsenide crystal. *J. Cryst. Growth* **65**, 166–172.

CROCHET, M. J., GEYLING, F. T. & SCHAFTINGEN, J. J. VAN 1987 Numerical simulation of the

horizontal Bridgeman growth. Part I: Two-dimensional flow. *Intl J. Numer. Meth. Fluids* **7**, 29–48.

DAVIS, S. H. & ROSENBLAT, S. 1977 On bifurcating solutions at low frequency. *Stud. Appl. Maths* **57**, 59–76.

EXTREMET, G. P., FONTAINE, J.-P., CHAOUCHE, A. & SANI, R. L. 1990 Two- and three-dimensional finite element simulations of buoyancy-driven convection in a confined Pr=0.015 liquid. In *Numerical Simulation of Oscillatory Convection in Low-Pr Fluids* (ed. B. Roux). Notes on Numerical Fluid Mechanics, vol. 27, pp. 171–181. Vieweg.

FILYAND, M. A. & SEMENOVA, E. I. 1968 *Handbook of the Rare Elements, Vol.1: Trace Elements and Light Elements.* MacDonald Technical and Scientific.

GARREC, S. LE & MAGNAUD, J. P. 1990 Numerical simulation of oscillatory convection in low Prandtl fluids. In *Numerical Simulation of Oscillatory Convection in Low-Pr Fluids* (ed. B. Roux). Notes on Numerical Fluid Mechanics, vol. 27, pp. 189–198. Vieweg.

GERVASIO, C., BOTTARO, A., AFRID, M. & ZEBIB, A. 1990 Oscillatory natural convection in a long horizontal cavity. In *Numerical Simulation of Oscillatory Convection in Low-Pr Fluids* (ed. B. Roux). Notes on Numerical Fluid Mechanics, vol. 27, pp. 136–143. Vieweg.

GILS, S. A. VAN, KRUPA, M. & LANGFORD, W. F. 1990 Hopf bifurcation with non-semisimple 1:1 resonance. *Nonlinearity* **3**, 825–850.

GOLUBITSKY, M. & LANGFORD, W. F. 1981 Classification and unfoldings of degenerate Hopf bifuractions. *J. Diffl Equat.* **41**, 375–415.

GUCKENHEIMER, J. & HOLMES, P. 1983 *Nonlinear Oscillations, Dynamical Systems, and Bifurcations of Vector Fields.* Springer.

HAMPEL, C. A. 1954 *Rare Metals Handbook.* Reimhold.

HART, J. E. & PRATTE, J. M. 1990 A laboratory study of oscillations in differentially heated layers of Mercury. In *Numerical Simulation of Oscillatory Convection in Low-Pr Fluids* (ed. B. Roux). Notes on Numerical Fluid Mechanics, vol. 27, pp. 329–337. Vieweg.

HENRY, D. & BUFFAT, M. 1990Two and three-dimensional numerical simulations of the transition to oscillatory convection in low-Prandtl number fluids. Prepublication.

HULTGREN, R. ET AL. 1973 *Selected Values of the Thermodynamic Properties of the Elements.* ASM.

HURLE, D. T. J. 1966 Temperature oscillations in molten metals and their relationship to growth striae in melt-grown crystals. *Phil. Mag.* (8) **13**, 305–310.

HURLE, D. T. J., JAKEMAN, E. & JOHNSON, C. P. 1974 Convective temperature oscillations in molten Gallium. *J. Fluid Mech.* **64**, 565–576.

IIDA, T. & GUTHRIE, R. I. L. 1993 *The Physical Properties of Liquid Metals.* Clarendon.

KAYE, G. W. C. & LABY, T. H. 1982 *Tables of Physical and Chemical Constants*, 14th edn. Longman.

KOBINE, J. J., MULLIN, T. & PRICE, T. J. 1995 The dynamics of driven rotating flow in a stadium-shaped domains. *J. Fluid Mech.* **294**, 47–69.

LANGE, N. A. 1967 *Handbook of Chemistry*, revised 10th edn. McGraw-Hill.

LANGLOIS, W. E. 1985 Buoyancy-driven flows in crystal-growth melts. *Ann. Rev. Fluid Mech.* **17**, 191–215.

MCKELL, K. E., BROOMHEAD, D. S., JONES, R. & HURLE, D. T. J. 1990 Torus doubling in convecting molten Gallium. *Europhys. Lett.* **12**, 513–518.

MÜLLER, A. & WIEHELM, M. 1964 Periodische Temperaturschwankungen in flüssigem InSb als Ursache schichtweisen Einbaus von Te in Kristallisierendes InSb. *Z. Naturf.* A **19**, 254–263.

MULLIN, T. (ed.) 1993 *The Nature of Chaos.* Clarendon.

OKADA, K. & OZOE, H. 1993 The effect of aspect ratio on the critical Grashof number for oscillatory natural convection of zero Prandtl number fluid; numerical approach. *J. Cryst. Growth* **126**, 330–334.

PIMPUTKAR, M. & OSTRACH, S. 1981 Convective effects in crystals grown from melts. *J. Cryst. Growth* **55**, 614–646.

PRATTE, J. M. & HART, J. E. 1990 Endwall driven, low Prandtl number convection in a shallow rectangular cavity. *J. Cryst. Growth* **102**, 54–68.

PULICANI, J. P., DEL ARCO, E. C., RANDRIAMAMPIANINA, A., BONTOUX, P. & PEYRET, R. 1990 Spectral simulations of oscillatory convection at low Prandtl number. *Intl J. Numer. Meth. Fluids* **10**, 481–517.

LE QUÉRÉ, P. 1990 Contribution to the GAMM Workshop with a pseudo-spectral Chebyshev

algorithm on a staggered grid. In *Numerical Simulation of Oscillatory Convection in Low-Pr Fluids* (ed. B. Roux). Notes on Numerical Fluid Mechanics, vol. 27, pp. 227–236. Vieweg.

ROUX, B. (ed.) 1990 *Numerical Simulation of Oscillatory Convection in Low-Pr Fluids.* Notes on Numerical Fluid Mechanics, vol. 27. Vieweg.

ROUX, B., BEN HADID, H. & LAURE, P. 1989 Hydrodynamical regimes in metallic melts subject to a horizontal temperature gradient. *Eur. J. Mech.* B **8**, 375–396.

THEVENARD, D., ROUZAUD, A., COMERA, J. & FAVIER, J. J. 1991 Influence of convective thermal oscillations on a solidification interface in Bridgeman growth. *J. Cryst. Growth* **108**, 572–582.

TOULOUKIAN, Y. S. ET AL. (eds.) 1979 *Thermophysical Properties of Matter, Vol.1: Thermal Conductivity: Metallic Elements and Alloys.* The TPRC Data Series. IFI/Plenum.

WEAST, R. C. (ed.) 1983 *CRC Handbook of Chemistry and Physics*, 64th edn. CRC.

WEAST, R. C. (ed.) 1993 *CRC Handbook of Chemistry and Physics*, 74th edn. CRC.

WIGGINS, S. 1990 *Introduction to Applied Nonlinear Dynamical Systems and Chaos.* Springer.

WINTERS, K. H. 1988 Oscillatory convection in liquid metals in a horizontal temperature gradient. *Intl J. Numer. Meth. Engng* NSI, pp. 401–414.

WINTERS, K. H. 1990 A bifurcation analysis of oscillatory convection in liquid metals. In *Numerical Simulation of Oscillatory Convection in Low-Pr Fluids* (ed. B. Roux). Notes on Numerical Fluid Mechanics, vol. 27, pp. 319–326. Vieweg.

WINTERS, K. H. & JACK, R. O. 1989 Anomalous convection at low Prandtl number. *Commun. Appl. Numer. Meth.* **5**, 401–404.